XL CILAMCE
IBERO-LATIN AMERICAN CONGRESS ON COMPUTATIONAL METHODS IN ENGINEERING
NOVEMBER 11-14, 2019
Praiamar Natal Hotel & Convention Natal, RN-BRAZIL

SIMULATION OF GENERATION AND PROPAGATION OF TENSILE FRACTURES IN LAMINATED CARBONATES OF THE CRATO FORMATION CONSIDERING STRATIGRAPHIC HETEROGENEITY

Ana Itamara Paz de Araújo
Igor Fernandes Gomes
anaitapaz@hotmail.com
gomes@ufpe.br
Department of Civil Engineering, Federal University of Pernambuco
Recife, Pernambuco 50670-901, Recife-PE-Brazil
Tiago Siqueira Miranda
Antônio José Barbosa
tiagogeoufpe@gmail.com
barboant@hotmail.com
Department of Geosciences, Federal University of Pernambuco
Recife, Pernambuco 50670-901, Recife-PE-Brazil

Abstract. The Crato-PE Fm is part of the Araripe Basin, being one of the largest areas in relation to the interior basins of north e astern Brazil. This led to the reactivation of old paddles for inversions, and converting an old graven into a horst. This work seeks to simulate numerically a generation and propagation of natural fractures for the effect of vertical lithological variation on fractures. In the present work, it is proposed the use of the technique of fragmentation of high aspect ratio mesh elements to model, together with the constitutive model of Damage to traction, a generation and propagation of fractures. This type of model is able to divert the effect of the materials when submitted to progressive processes of mechanical degradation by reducing the rigidity of the material. The problem analysed is the simulation of the generation and propagation of extension fractures in a profile considering interleaving of laminate layers with other types of lithology's, representing a faciological variation with impact on the mechanical competence of the layers on the genesis and propagation of the extension fractures. In order to perform the study of fracture generation and propagation, we used the fragmentation technique with special interface finite elements. This technique was chosen because it numerically represents the behaviour of intensively fractured media, in which the special interface elements are located between the regular finite elements. Was considered submitted to a vertical tension representing a vertical burial state, and a horizontal tension variation the extension direction. The base and one of the lateral borders of the domain are restricted as to the displacement in the normal direction. The analysis is in flat deformation considering a Lagrangean approach for the deformations. It has been found that as the prescribed tensile stress on the left side of the section increases, horizontal tensile stresses develop in the layers, but with a higher concentration in the laminate layer of greater stiffness and tensile strength.

Keywords: Fm. Crato, Propagation, Generation and Fractures.

1 Introduction

The Araripe Basin is located in the Borborema Transverse Zone Domain (PB), as is the Duck Shear Zone (ZCPA). The BA suffered an inversion, the result of an exposure between the meso-Atlantic chain with the Andes, which caused a transition from an extensional regime to a compressional regime. This led to the reactivation of old paddles for inversions, and converting an old graben into a horst. The effect of the compressional regime on the preexisting layers was the arching of the qualifying rocks, generating verticalized fractures along the stratigraphy of the formation being these influenced by the geomechanical heterogeneity of the rock features.

With this discovery of a thick layer of salt, called the Brazilian pre-salt, studies with the objective of oil exploration and production were necessary, these studies being of high complexity where one of the main difficulties is the heterogeneity of the formation, which occurs at multiple scales in the presence of several geological structures, such as fractures, faults, veins and karst features. Such conditions totally influence the prediction and production of gas and oil from the reservoir.

One of the artifices used to study and characterize the oil reservoir is to study similar outcrops that, according to Miranda *et al.* (2012), are characterized as rock formations that can be accessed on the surface and which resemble similar exploratory targets in subsurface. Similar outcrops of reservoirs exist for almost all subsurface reservoir geometries (Geiger & Matthai, 2012).

Because of the difficulty of capturing logs of underground images, outcrops are an opportunity to investigate the characteristics of fractures. This is applied, especially the dimensions of fractures and the relationships of connectivity between them, and the orientation and evaluation of fracture networks and their general aspects can also be studied (Mercadier & Makel, 1991; Van Dijk 1998).

Therefore, an analogous lithophaciological outcrop is proposed that is closer to the geological characteristics of the reservoir to be developed. These characteristics, such as fracture and failure systems, because their importance is great in relation to the storage and flow of fluids, which occur in naturally fractured reservoirs represents an important aspect, especially for carbonate reservoirs (SANTOS, 2017).

In this article the analogous outcrop that will be studied is a laminated limestone located in the Crato Formation. This outcrop has been used with the objective of studying reservoirs in the pre-salt range of the Santos and Campos Basins, in the southeast margin of the country (CATTO *et al.*, 2016; MIRANDA, 2015; SANTOS *et al.*, 2017; ZIHMS, 2017; Miranda *et al.*, 2018). This outcropping was chosen due to the easy access to laminated limestone outcrops reaching up to 20 meters high and up to hundreds of meters of lateral exposure (ALENCAR, 2018).

2 Araripe Basin and Crato Formation

The Crato Formation is located in the Araripe Basin (BA), which has an extension of approximately $9.000 km^2$, being the largest area in relation to the basins of the interior and northeastern Brazil. Figure 1 shows the simplified map of the Araripe Basin.

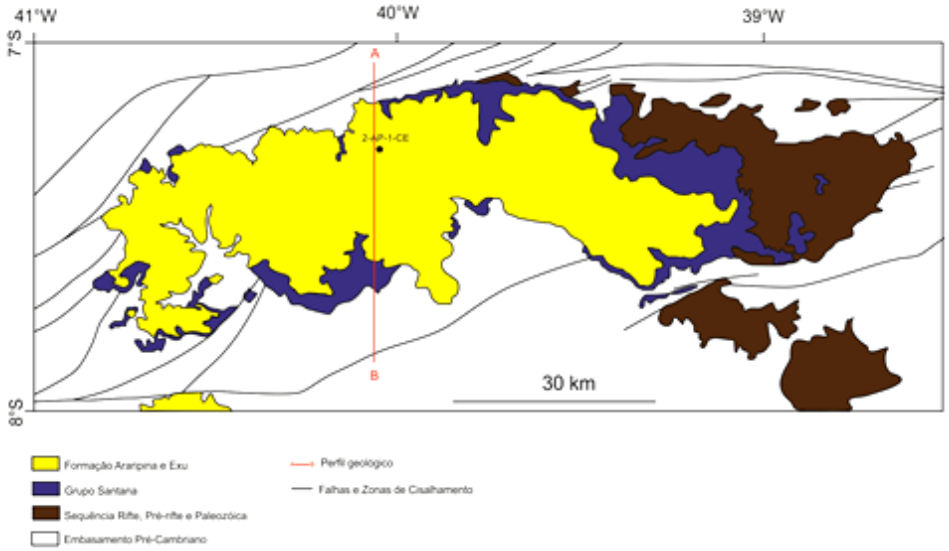

Figure 1. Simplified map of the Araripe Basin.
Font. Adapted from Assine, 2007.

The evolution of the Basin can be explained through Figure 2 which follows.

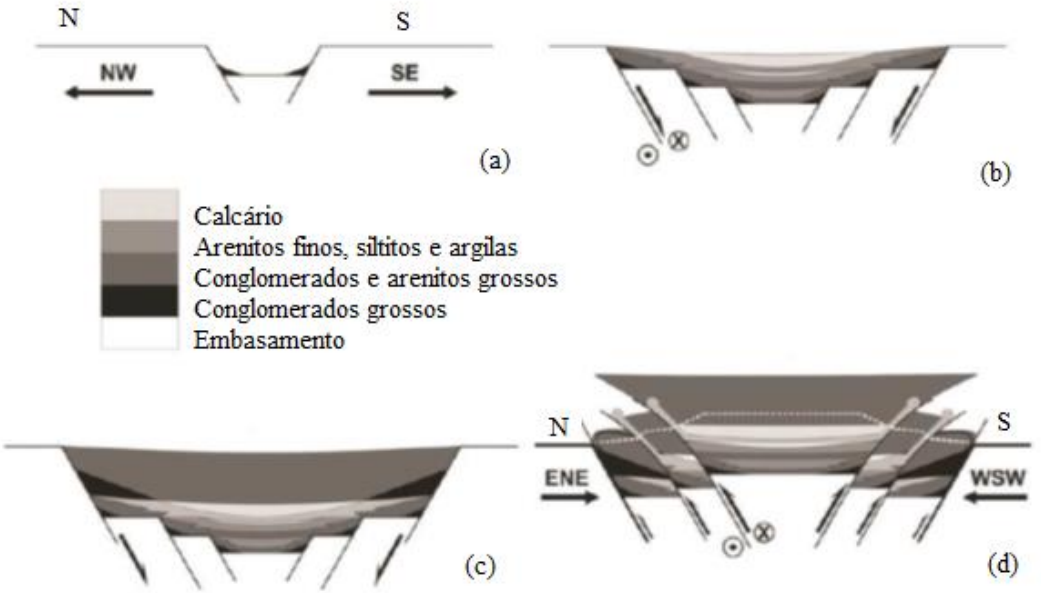

Figure 2. (a) Beginning of the rift, from a narrow graben; (b) widening and deepening of the rift, from basement failure; (c) Final stage of the rift, contemporary with the opening of the Atlantic; (d) Inversion of the basin due to oblique compression efforts, with the injection of ductile rocks through the normal reactivated faults, and the reduction of inverted faults. The white dashed line indicates the current topography of the basin, with the plateau.
Font. Marques *et al.*, 2014.

The Crato Formation has features of shear fractures, stylolite, extension fractures and vugular fractures (Miranda, 2015). In this thesis, the focus will be to simulate the occurrence of extension fractures, since it is these fractures that have the highest frequency of occurrence in the limestone's of the Crato Formation. The Figure 3 shows the data acquisition profile for the study of mechanical stratigraphy of laminates in outcropping of the Fm. Crato.

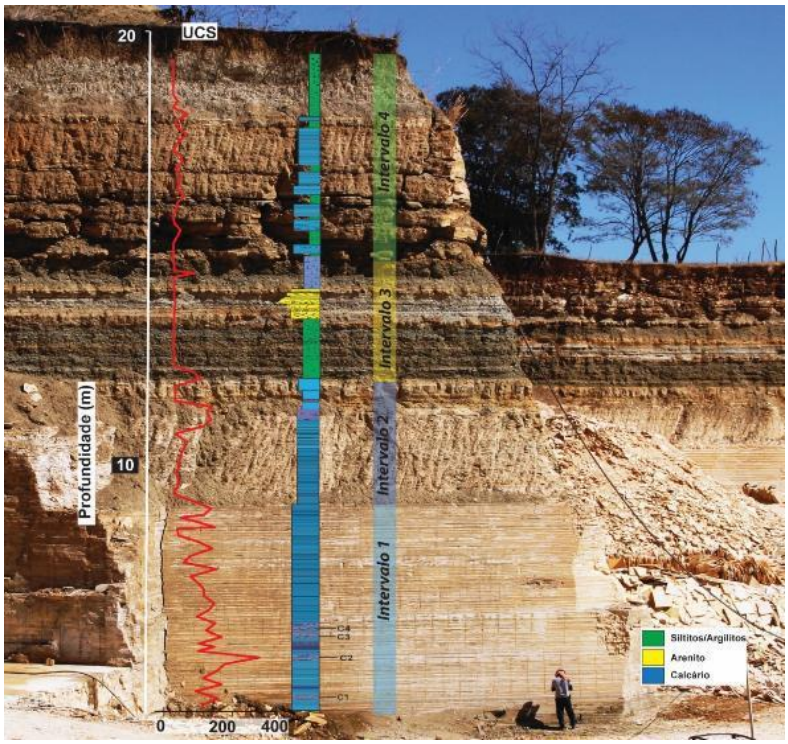

Figure 3. Data acquisition profile for the study of mechanical stratigraphy of laminate's in outcropping of Fm. Crato, at Três Irmãos Mine: Variation of mechanical face's.
Font. Project Report Crato / UFPE / Petrobras, 2017.

3 Constitutive model of traction damage

Based on the mechanics of continuous damage, proposed by Simó & Ju (1987), the damage is a degradation of the rigidity of the material. Therefore it is understood that the model is based on the irreversible thermodynamic processes and is proposed in a way that describes the previous mechanism of the formation of macro fractures.

In the case of Traction Damage, Oliver *et al.*, (2008) introduced to the damage model, treating the material differently when subjected to a state of traction or compression. The formulation described in this thesis can be found more broadly in Sánchez *et al*., (2014) which treated that when the material is in the compressive state it will have linear elastic behavior.

And when the damage is in the regime of traction to the constitutive equations will be described introduced the concept of effective tension of damage in order to describe the behavior of the damaged environment.

As described by Sánchez *et al.*, (2014), the constitutive law of this model is described as follows:

$$\sigma = (1 - d)\bar{\sigma} \tag{1}$$

Since σ is the effective stress, d is the damage variable $(0 \leq d \leq 1)$ and $\bar{\sigma}$ is the effective stress of damage, which is given by:

$$\bar{\sigma} = \boldsymbol{C} : \varepsilon \tag{2}$$

Where $\boldsymbol{C}$ is the tensile constitutive elastic. Thus, the constitutive law for this model can be expressed by:

$$\sigma = (1 - d)\bar{\sigma}, \ if \ \overline{\sigma_n} > 0 \quad \text{Tensile state}$$

$$\sigma = \bar{\sigma}, \quad if \ \overline{\sigma_n} \leq 0 \quad \text{Compression state} \tag{3}$$

4 Mesh fragmentation and finite interface elements

In the finite element technique with special interface elements of high aspect ratio (fragmentation) the normal direction is defined as being at the base of the interface element, as shown in Figure 4.

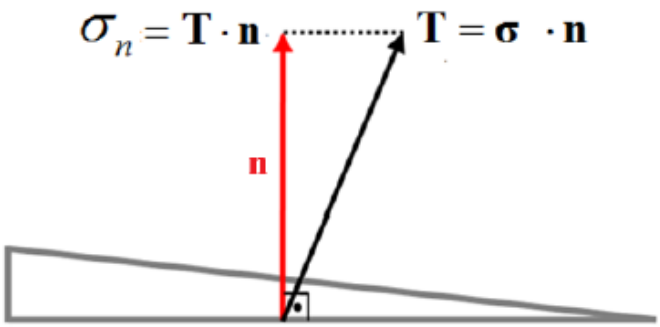

Figure 4. Projection of the vector of voltages in the normal direction the base of the interface element.
Font. Sánchez *et al.*, 2014.

The peculiarity of the used element that composes the interface is a linear triangle with high aspect ratio, whose kinematics is compared with the kinematics of the approximation of strong discontinuities in modeling mechanical problems. Figure 5 shows the steps of the fragmentation of a conventional finite element mesh. The purpose of such a technique is to use a thickness less than the finite element thickness located in the continuous medium. For as the thickness (*h*) decreases the aspect ratio increases, resulting in a kinematics similar to what can be observed in the kinematics of the Continuous Approach to Strong Discontinuities (ACDF).

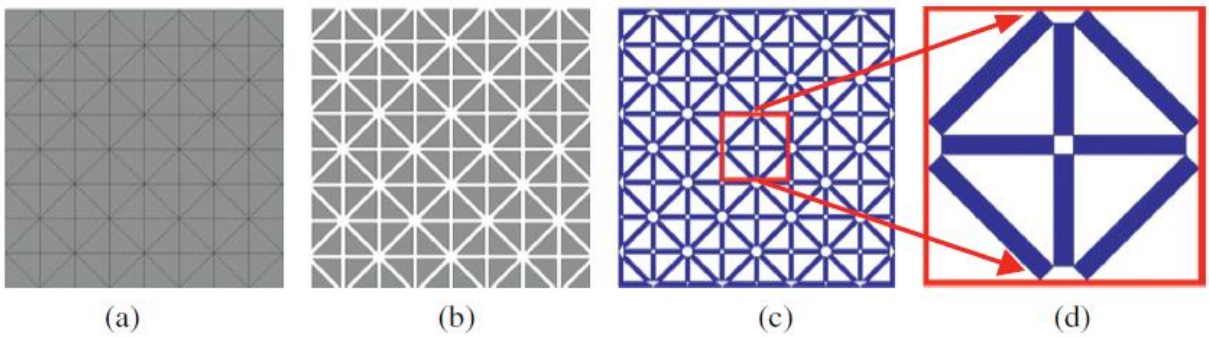

Figure 5. Main steps associated with the mesh fragmentation technique. (a) Conventional finite element mesh; (b) Fragmentation of the mesh; (c) Insertion of elements of high aspect ratio; (d) Detail of interface elements.
Font. Sánchez *et al.*, 2014.

In this way the mesh that passes through the fragmentation process will have in its composition regular finite elements, which represent the continuous medium or the non-fractured material, and finite interface elements representing the discontinuities or the possible paths for the opening of fractures in the medium.

5 Numerical simulations analogues outcrop mesh fragmentation

The simulation consists of simulating the formation, generation and propagation of natural fractures in a two - dimensional section representative of a stratigraphic profile of the Fm. Crato considering the effect of layer heterogeneity. The objective was to analyze the effect of mechanical

properties differences (Young's modulus and tensile strength) of each layer on the generation and propagation of fractures, given a lateral extensional regime, to simulate the bowing effect of the basin, and vertical compression for simulate the burial of the Fm. Crato by the other Formations.

It was elaborated conceptually, based on the study of mechanical stratigraphy of the Fm. Crato conducted by the geology team of the Crato UFPE / Petrobras project, carried out to the top of the C6 level of this required Formation, along the lithological profile PC-0. In this, four lithology intervals with different elastic resistance values were measured, measured with UCS (Uniaxial Compressive Strength) in situ measurement.

Therefore, the scenario analyzed consists of a hypothetical profile composed of 5 layers with different mechanical properties, such as the modulus of elasticity, Poisson's coefficient and tensile strength of the rock. Thus, a vertical section (2D) representative of the Fm. Crato. The profile is subjected to a vertical displacement rate of $(-7.00076e^{-9}m/s)$, representing a vertical burial state, and a horizontal displacement rate variation of $(0\ a\ -1.8103^{-8}m/s)$, in the sense of extension, as shown in Figure 6, which also shows the constraint boundary conditions at the base and edge of the domain. This analysis was in flat deformation.

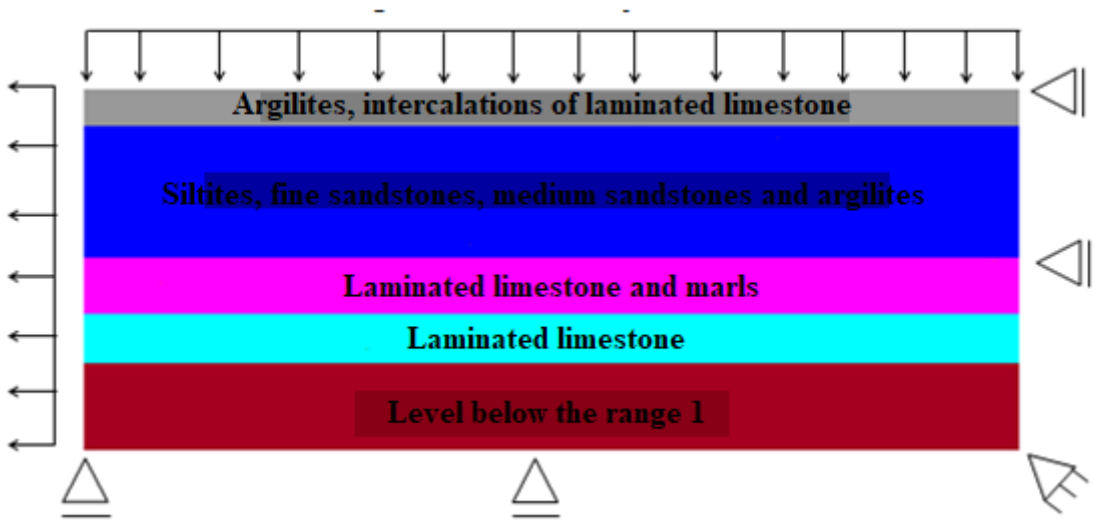

Figure 6. Domain detail and boundary conditions.

The finite element mesh presents 55525 nodes and 64606 elements, composed of elements of the linear triangle type and considering the application of the fragmentation technique that inserts finite elements with high aspect ratio. These elements have an initial thickness of 1.0x10-5 m. The constitutive model adopted is the Traction Damage model with fault criterion that assumes the propagation of the fracture in the direction of maximum tensile tension. The damage model was applied only to the interface elements, being a linear elastic model associated with regular finite elements. Figure 7 shows the mesh and their respective materials, being five types of features and fifteen materials containing the finite elements of special interface, provided constitutive relations suitable to represent the effects of the fracturing process.

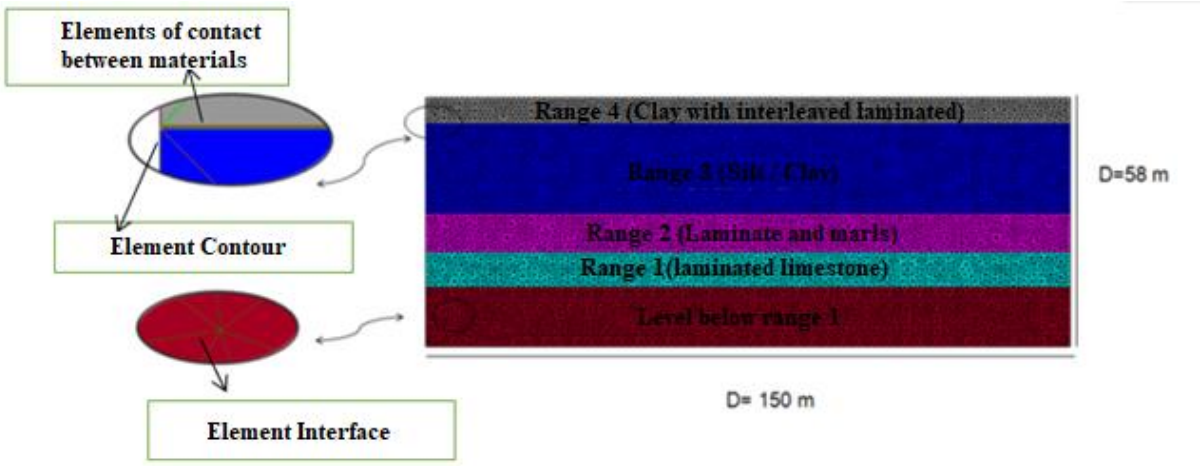

Figure 7. Detailing the domain and the finite element mesh.

Table 1 presents the properties used in the analysis, being the modulus of elasticity (E), Poisson Coefficient (ν) and tensile strength (δ_y) of each material of this simulation. The fracture energy (G_F) adopted was 100 N/m. The ordering of the layers occurs from top to bottom. Layer four, interval 1, consists of a laminate of greater rigidity.

Table 3. Properties of the materials used in the profile of extension fractures in profile.

Materials	Modulus of Elasticity $(E)GPa$	Poisson (ν)	Fracture Energy $G_f N/m$	Tensile Strength $(\delta_y)MPa$
Interval 4 (continuous)	24000.00	0.247	-----	Elastic
Interval 4 (Interface)	24000.00	0.247	100.00	8.50
Interval 3 (continuous)	24000.00	0.247	-----	Elastic
Interval 3 (Interface)	24000.00	0.247	100.00	9.00
Interval 2 (continuous)	25000.00	0.247	-----	Elastic
Interval 2 (Interface)	25000.00	0.247	100.00	9.05
Interval 1 (continuous)	26000.00	0.247	-----	Elastic
Interval 1 (Interface)	26000.00	0.247	100.00	9.10
Base (continuous)	24500.00	0.247	-----	Elastic
Base (Interface)	24500.00	0.247	100.00	9.00

The distribution of the horizontal stresses (direction of extension) in the domain is presented. It was verified that as the prescribed displacement rate on the left side is applied horizontal tensile stresses develop in the layers, but with a higher concentration in layer 04 consisting of the laminate of greater rigidity and tensile strength. This is because the other layers, in relation to this, suffer greater deformation before the rupture.

Figure 8 shows the distribution of the horizontal stress immediately before and immediately after the rupture, with the recurrence of fracture generation. Once the stresses reach the value of tensile strength of the rock, the fractures are generated and there is a relief of stresses in the layer. A stress concentration at the tips of the fractures is observed, showing its interaction with the capping layer.

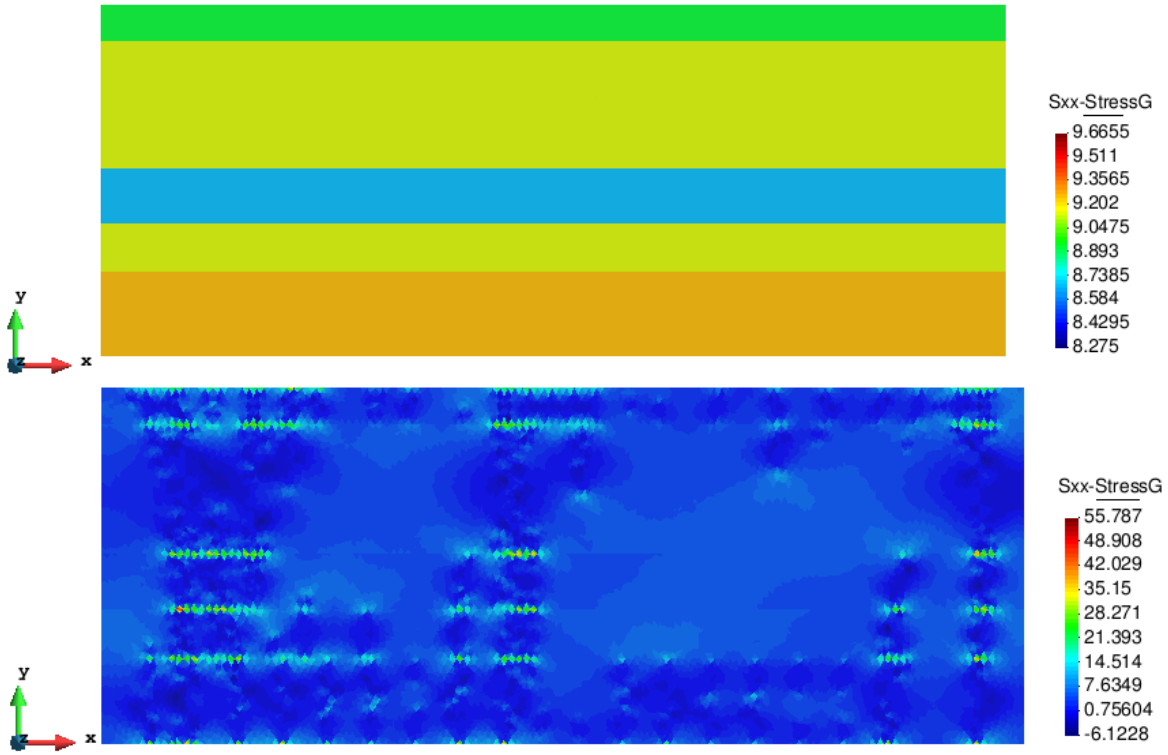

Figure 8. Distribution of horizontal stresses. (a) Instant before fracture generation; (b) Moment after generation of fractures.

Given the state of tensions reached, the material suffers damage in localized regions and thus the damage variable reaches the unit and the interface element has its degenerate stiffness and its aperture increased, thus configuring a jump in the field of displacements and the formation of a fracture.

This can be observed in Figure 9 where graphically shows the evolution of the horizontal voltage variation curve with time for points adjacent to fractures in different regions of the features. It is verified that the voltage at which the total rupture occurs varies in a range of 8.65 and 9.1MPa, which is in agreement with the tensile strength imposed in the conditions of the problem.

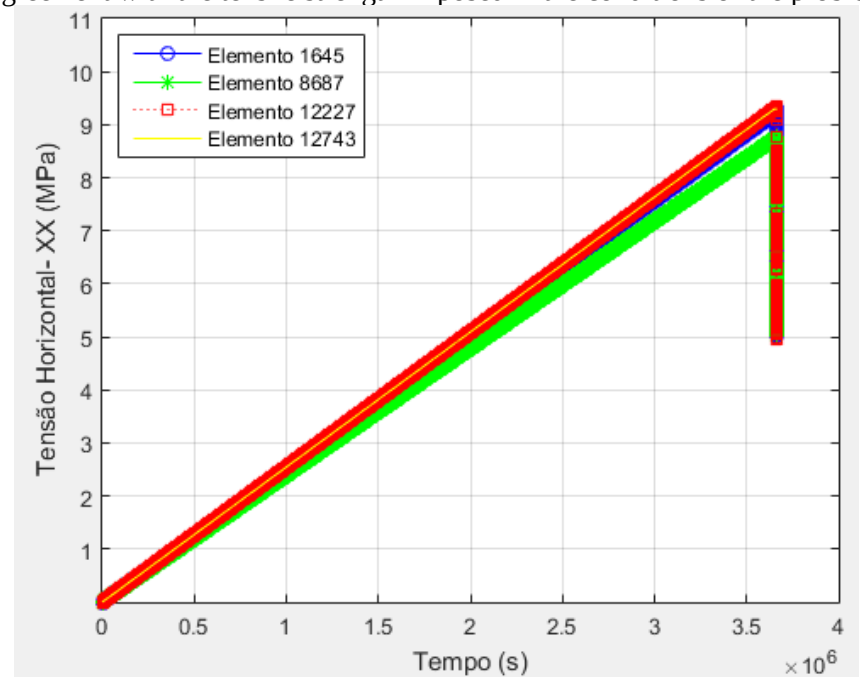

(a)

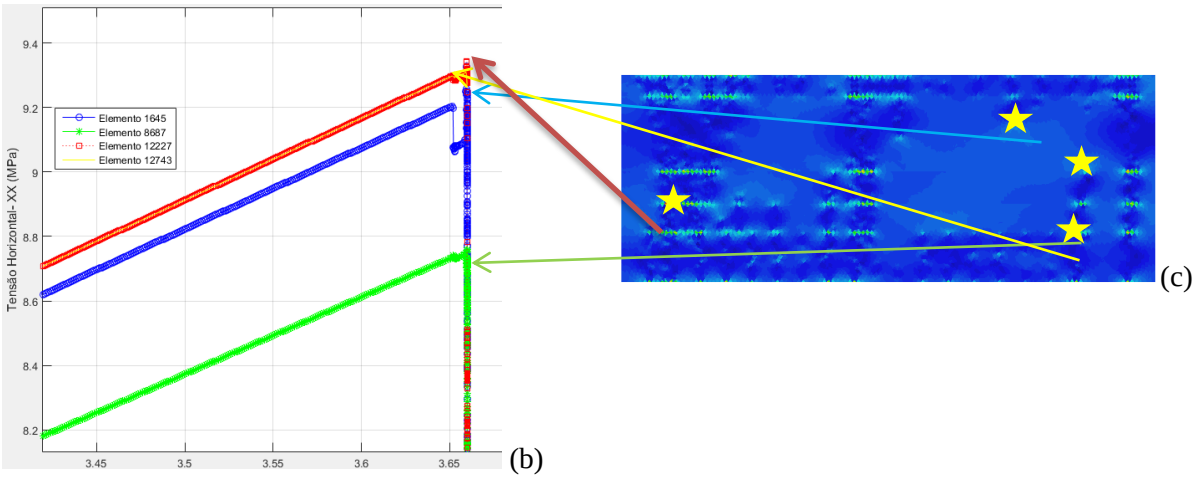

Figure 9. Evolution of the horizontal stress curve. (a) Graph of the evolution of horizontal stresses with respect to time; (b) Zoom of the graph of horizontal stresses; (c) Location of the elements.

This study of the evolution of horizontal stresses, to study the effect of rupture of the material, is presented Figure 10 shows the damage variable assuming unit value. However, since this occurs only in the interface elements, whose thickness is very small compared to the dimensions of the domain, applying a factor of magnification (scale) in the deformed finite element mesh, such elements can be visualized in red colour. In this way it is possible to visualize the generated fractures and their propagations.

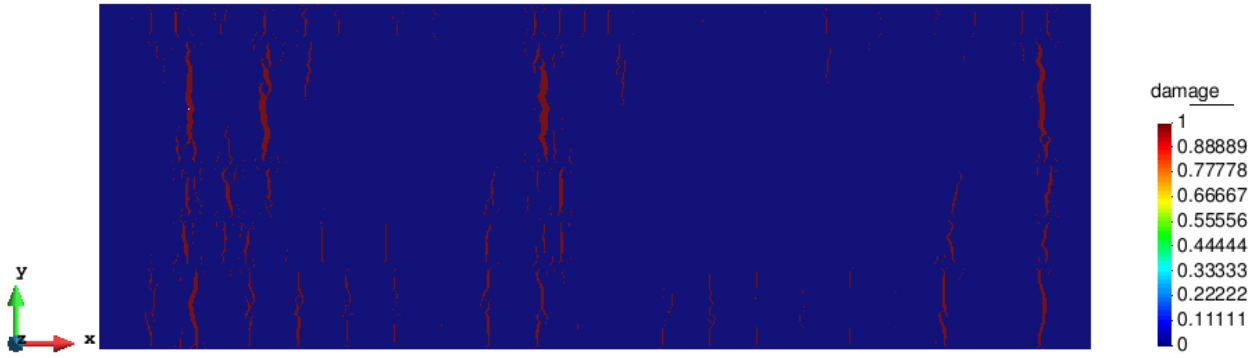

Figure 10. Variable damage with magnification factor 80 times.

Figure 11 presents a detail of the most representative fractures (of greater aperture and visually identifiable), considering the identification of each layer. It is possible to observe the propagation of the fractures in the layers above and below the most competent rock, but with a relative displacement (translation of the fracture line). In addition, there are fractures with smaller openings from which it is also possible to visualize.

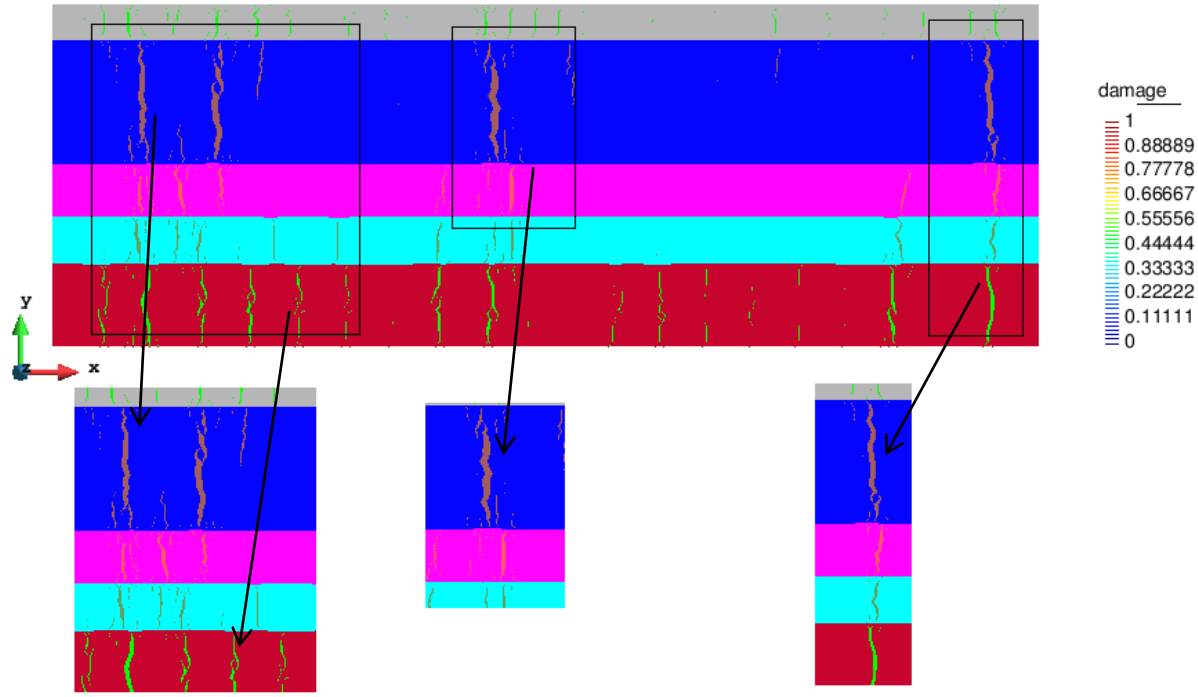

Figure 11. Detail of a sample of the fractured region: Interaction of the fractures generated in the 02 and 04 with the layers of base and sealant (black arrows indicating visible fractures).

By numerically obtaining the fracture patterns that occur in this symmetric profile of the Fm. Crato, adding to the study of mechanical stratigraphy performed by the geology team at the Crato UFPE / Petrobras Project, information was obtained on the influence of the heterogeneities of the laminates of the Fm. Crato (concretions, lamination, faciological variation) through in situ geomechanical characterization using acquisitions of effective elasticity related to the fracturing intensity.

It was observed the occurrence of confined fractures in layers of laminate itself whose variation of stiffness was observed as a function of the roughness observed in the wall of the sub layer. Figure 12 is an example of this type of observation, on a scale of centimetre's, on the laminate of Fig. Crato. It is observed the generation and confinement of fractures in some layers due to the vertical variation of geomechanical properties.

Figure 12. Data acquisition profile for mechanical stratigraphy study of laminites of Fm. Crato, location of extension fractures along the profile with prominence for confined fractures in layers 1 and 2. Font. Report Project Crato / UFPE / Petrobras, 2017.

Taking into account the scale of the mechanical stratigraphy used to construct the model, to the top of the C6 level along the lithological profile PC-0, it is observed in Figure 13 the delimitation, confinement, of existing fractures between two lithology intervals.

Truncation of the fracture of the lower layer and a bifurcation of this layer and interruption in the upper layer is observed. This same type of pattern was observed in the numerical analyses presented.

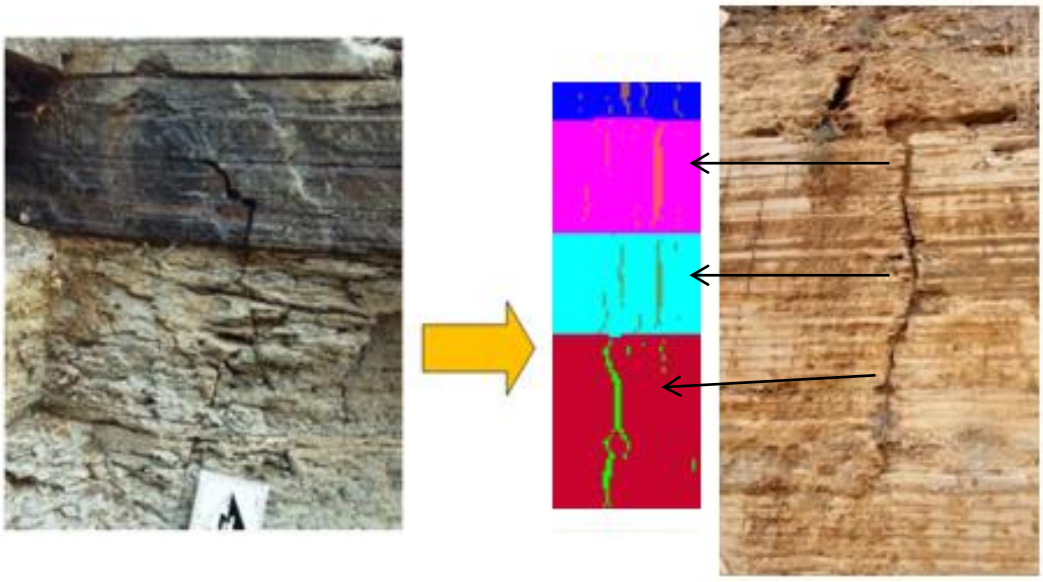

Figure 13. Propagation of fractures between different mechanical intervals.
Font. Adapted from Project Report Crato / UFPE / Petrobras, 2017.

6 Conclusions

The simulation was able to capture the pattern of fractures distributed in the Crato formation, so the simulation considers the variation of features and depth where the numerical response proved to be compatible with that of outcropping, where mechanical features present a higher density of fractures in the fragile / ductile deformation before rupture, this leads to a process of fracture generation and with propagation in which some fractures are truncated by the features and with displacement between one feature and another (effect *en échelon*). Therefore, this result validates the simulation of generation and propagation of fractures of the Crato Formation.

Acknowledgements

To the GeomeCCarb research project: Study of Geomechanical and Geochemical Couplings in Carbonate Reservoirs, for financial support. The Laboratory of Computational Methods in Geomechanics for the support for the development of this work.

References

Alencar, Márcio L. **Caracterização dos estilólitos verticais do nível superior dos calcários laminados da formação Crato, borda norte da Bacia do Araripe.** 2018. Dissertação (Mestrado) - Universidade Federal de Pernambuco, Recife, 2018.

ASSINE, M. L., 2007, Bacia do Araripe: Boletim de Geociências da Petrobras, v. 15, p. 371–389.

CATTO, B., Jahnert, R. J., Warren, L. V., Varejão, F. G., Assine, M. L.. 2016. **The Microbial Nature of Laminated Limestones: Lessons from the Upper Aptian, Araripe Basin, Brazil.** Sedimentary Geology 341: 304-315. Doi: 10.1016/j.sedgeo.2016.05.007.

GEIGER S., and Matthäi, S. **What can we learn from high-resolution numerical simulations of single- and multi-phase fluid flow in fractured outcrop analogues.** Geological Society, London, Special Publications published online September 5, 2012.

MERCADIER, C. G. & MAKEL, G. H. 1991. **Fracture patterns of Natih Formation outcrops and their implications for the reservoir modelling of the Natih field, North Oman**. Society of Petroleum Engineers Paper, 21377.

MIRANDA, T. S., R. F. Santos, J. A. Barbosa, I. F. Gomes, M. L. Alencar, O. J. Correia, T. C. Falcão, J. F. W. Gale, and V. H. Neumann, 2018. **Quantifying Aperture, spacing and fracture intensity in a carbonate reservoir analogue: Crato Formation, NE Brazil.** Marine and Petroleum Geology, v. 97, November 2018. P. 556-567.

MIRANDA, T., S.. 2015. **Caracterização Geológica e Geomecânica dos Depósitos Carbonáticos e Evaporíticos da Bacia do Araripe, NE Brasil**. Tese de Doutorado. 259p.

MIRANDA, T. S.; Barbosa, J.A.; Gomes, I. F.; Neumann, V. H.; Santos, R. F. V. C.; Matos, G.; Guimaraes, L. J. N.; Florencio, R. Q.; Alencar, M. L. Aplicação da Técnica de Scanline a Modelagem Geológica/Geomecânica de Sistemas de Fraturamento nos Depósitos Carbonáticos e Evaporíticos da Bacia do Araripe, NE do Brasil.. Boletim de Geociências da PETROBRAS (Impresso), v. 20, p. 305-326, 2012.

OLIVER, J. et al. **Two-dimensional modeling of material failure in reinforced concrete by means of a continuum strong discontinuity approach**. Comput. Methods Appl. Mech. Engrg, 197 (2008) 332-348.

SÁNCHEZ, M., MANZOLI, O. L.; GUIMARÃES, L. **Modeling 3-D desiccation soil crack networks using a mesh fragmentation technique**. Computers and Geotechnics, 62, 27–39.2014.

SANTOS, Rafael Fernandes Vieira Correia. **Análise estatística de parâmetros de sistemas fraturados aplicados à modelagem de fluxo**. Tese de doutorado, UFPE, Recife, 2017.
SANTOS, R. F., Miranda, T. S., Barbosa, J. A., Gomes, I. F., Matos, G., Gale, J., Neumann, V., Guimarães, L. J. 2015. **Characterization of natural fractures systems: analysis of uncertainty effects in linear scanline results**. AAPG Bulletin.

SIMO; JU. **Stress and strain based continuum damage models: I Formulation.** Int. J. Solids Struct, 15 (1987) 821–840.

VAN DIJK, J.-P. 1998. **Analysis and modelling of fractured reservoirs**. Society of Petroleum Engineers Paper, 50570.

ZIHMS, S. G., Miranda, T., Lewis, H., Barbosa, J. A., Neumann, V. H., Souza, J. A. B., Cruz Falcão, da T.. 2017. **Crato Formation laminites – a Representative Geomechanical Pre-salt Analogue.** 5th Atlantic Conjugate Margins Conference, Porto de Galinhas, Pernambuco, brazil, 22th – 25th August 2017.